ANALYSIS OF EXCITATIONS FROM THE WAVENUMBER POINT OF VIEW

F. Chevillotte[1] , F.-X. Bécot[1] and L. Jaouen[1]

[1] Matelys
1 rue Baumer, 69120 Vaulx-en-Velin, France
Email: fabien.chevillotte@matelys.com

ABSTRACT

When analyzing the effect of damping factor of a simple plate subjected to air-borne excitation, the effect of damping is well known. Its effect is mainly observed around the critical frequency. This observation is no longer valid when looking at other types of excitations (turbulent boundary layer, the point load, rainfall, tapping machine ...). The aim of this study is to analyze the contents of different excitations in the wave numbers domain and to compare the influence of the damping factor for various excitations. This study helps to clarify the understanding of the behavior of a system and especially the importance of damping factor regarding the considered excitation. The transfer matrix method is used as it is now able to account for (i) finite size using spatial window of the radiation efficiency, (ii) numerous excitations by using plane wave decomposition, and (iii) mechanical links between panels. Injected power, radiation efficiency and radiated power are examined for a simple plate under several excitations in order to examine the transmission loss. An example is given on a classical double wall partition with mechanical links (studs) and filled with glass wool. This configuration is interesting because it combines air-borne and solid-borne paths. In particular, it shown that the damping factor does not have the same impact on both transfer paths. This type of analysis gives new insights into the interpretation of a given system performance.

1 INTRODUCTION

When dealing with a sound and vibration problem, the data are generally represented in the frequency domain, sometimes in the time domain and rarely in the wavenumber domain. Representation in the wavenumber domain is not commonly used because it need a wavenumber mapping for each frequency f.
However, the analysis in the wavenumber space can be usefull to understand the functioning of a full system from the excitation to the radiated sound.

This work is focused on the response of multilayer systems under various excitations. For all configurations, systems are immerged in air at ambient conditions of temperature and pressure. Each excitation (or load $f(x, y)$) can be represented as an infinite number of plane waves $F(k_x, k_y)$ using the spatial Fourier transform.
Each quantity relative to the problem under consideration (excitation, structure response, radiation efficiency, radiated power) can be expressed in the wavenumber domain (k_x, k_y).
First some examples of wavenumber representation will be presented and then it will be shown how this representation can help to understand the functioning of a system, and more particularly the effect of the damping on the response of a system.

2 REPRESENTATION IN THE WAVENUMBER DOMAIN

Considering the radiated power on the reception side of a multilayer system submitted to an excitation on the emission side as depicted in Fig.1, this problem can be seen as a block diagram (see Fig.2) in wavenumber domain with:

- $F(k_x, k_y)$ the excitation,
- $SF(k_x, k_y)$ the response of the multilayer system which acts as a *structural* filter,
- $\sigma(k_x, k_y)$ the radiation efficiency linking the velocity of the system on the reception side $V_{rec}(k_x, k_y)$ to the radiated power $\Pi_{rad}(k_x, k_y)$ which can be seen as a *radiation* filter.

This representation is independent of the number of layers contained in the system.
Note that plane waves $F(k_x, k_y)$ may also be expressed in the polar coordinate system $F(k_r, \phi)$ as depicted in Fig.1.

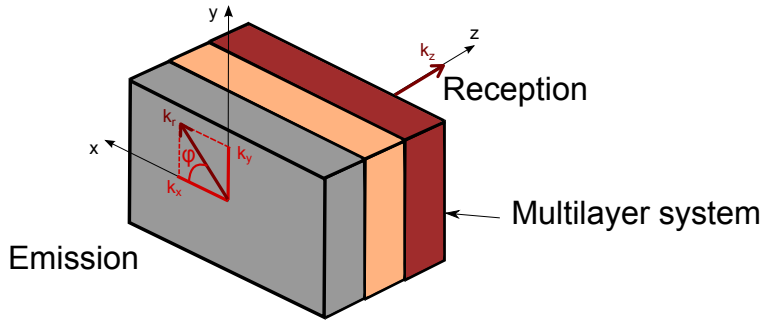

Figure 1. Multilayer system with spatial and wavenumber coordinates.

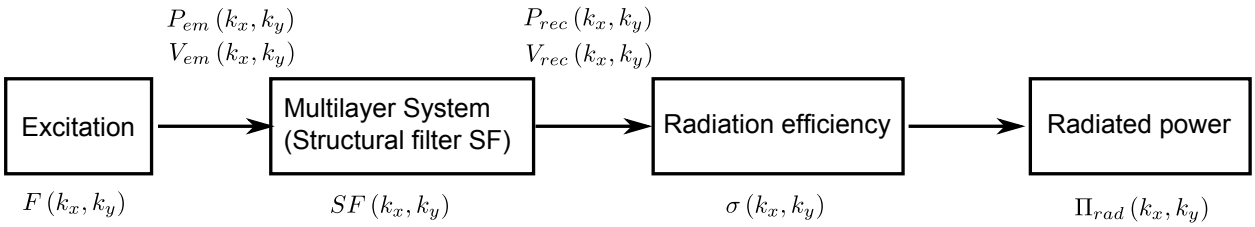

Figure 2. Block diagram of the problem.

First, some excitations, a structural filter and a radiation efficiency will be presented in the wavenumber domain.

2.1 Excitations

Air-borne diffuse field, structural load and turbulent boundary layer excitations are presented in the wavenumber domain at the frequency $f = 1000$ Hz. The acoustical wavenumber k_0 and the natural bending wavenumber k_b of a simple 4 mm thick aluminum plate are also plotted in the figures (Expression of k_b is given in Sec.2.2)
The acoustical wavenumber depends on the frequency f and the speed of sound in air c_0:

$$k_0 = \frac{2\pi f}{c_0}. \tag{1}$$

2.1.1 Air-borne excitation

In the particular case of a plane wave excitation with oblique incidence θ the polar/radial wave number k_r is defined for each frequency f as:

$$k_r = \sqrt{k_x^2 + k_y^2} = k_0 \sin(\theta) \tag{2}$$

This means that an oblique plane wave is represented in the 2D-wavenumber domain as a circle of radius k_r.
Representing a diffuse field excitation consists in an integration over θ from 0 to 90 degrees and corresponds to the area within a circle of radius k_0 as depicted in Fig.3. This illustrates the fact that for an air-borne excitation there is no energy in the wavenumber domain for k_r greater than k_0.

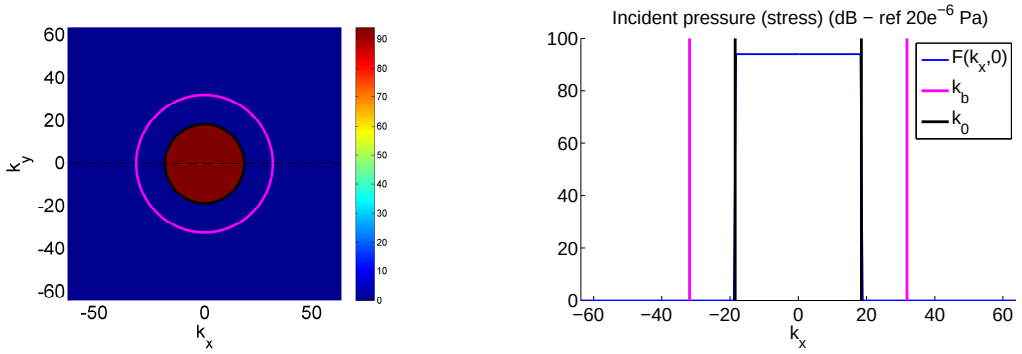

Figure 3: Example of air-borne diffuse field excitation at 1000 Hz in the wavenumber domain: 2D representation (left) and 1D representation along k_x (right).

2.1.2 Distributed structural load excitation

A distributed structural load of dimensions $L_x \times L_y$ in spatial domain is expressed as a multiplication of cardinal sine in the wavenumber domain where the zeros are multiple of $2\pi/L_x$ for k_x, and $2\pi/L_y$ for k_y.
If the dimensions L_x and L_y tend to 0, this excitation tends to a point force and the first zero $2\pi/L_x$ (or $2\pi/L_y$) is moved toward very high wavenumber values. This distributed structural load excitation is illustrated for $L_x \times L_y = 0.1 \times 0.1$ m^2 m in Fig.4.

2.1.3 Turbulent boundary layer excitation

The turbulent boundary layer is computed using the spatial correlation proposed by Corcos [1] and the empiral auto-spectra model as proposed by Goody [2]. The main characteristic of this excitation is a large convective peak around the convection wavenumber k_c. Moreover the excitation is

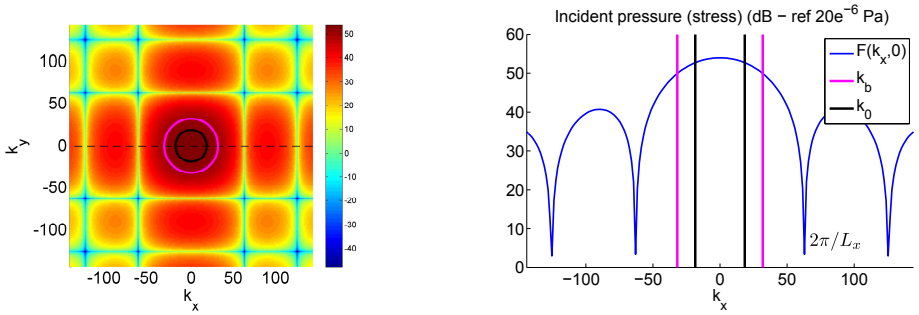

Figure 4: Example of distributed structural load excitation of width $L_x \times L_y = 0.1 \times 0.1$ m^2 at 1000 Hz in the wavenumber domain: 2D representation (left) and 1D representation along k_x (right).

asymmetric in the wavenumber domain.
The convection wavenumber is expressed as:

$$k_c = \frac{2\pi f}{U_c}, \tag{3}$$

where U_c is the convection velocity.

An illustration is given Fig.5 with a flow along the x-direction, a convection velocity of 100 m.s^{-1} and a boundary layer thickness of 0.025 m at the frequency $f = 1000$ Hz ($k_c = 62.8$ rad.m^{-1}).

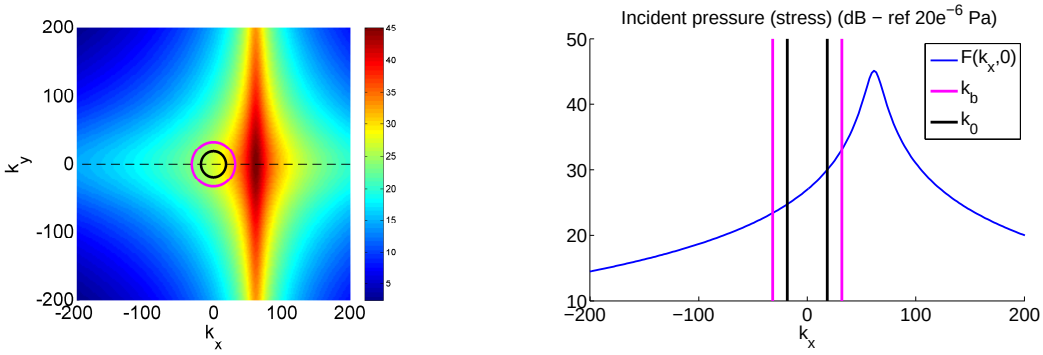

Figure 5: Example turbulent boundary layer excitation for a velocity $U_c = 100$ m.s^{-1} at 1000 Hz in the wavenumber domain: 2D representation (left) and 1D representation along k_x (right).

2.2 Structural filter

The excited multilayer system acts as a filter. For each wavenumber (k_x, k_y), the radiation problem can be solved using transfer matrix method [3, 4] linking pressure (or stress) P_{em} and velocity V_{em} on the emission side to P_{rec} and V_{rec}, pressure and velocity on the reception side. Note that the global condensed matrix $\mathbf{T}$ is 2×2 but this method allows to account for fluid, solid, poro-elastic layers. In the latter cases, the constitutive transfer matrices are larger than 2×2 matrices.
At this stage the multilayer system is assumed to be of infinite extent.

$$\begin{bmatrix} P_{em} \\ V_{em} \end{bmatrix} = \mathbf{T} \begin{bmatrix} P_{rec} \\ V_{rec} \end{bmatrix}, \tag{4}$$

The wavenumber filter of a simple 4 mm thick aluminum plate is represented in Fig.6 for two damping factor values.

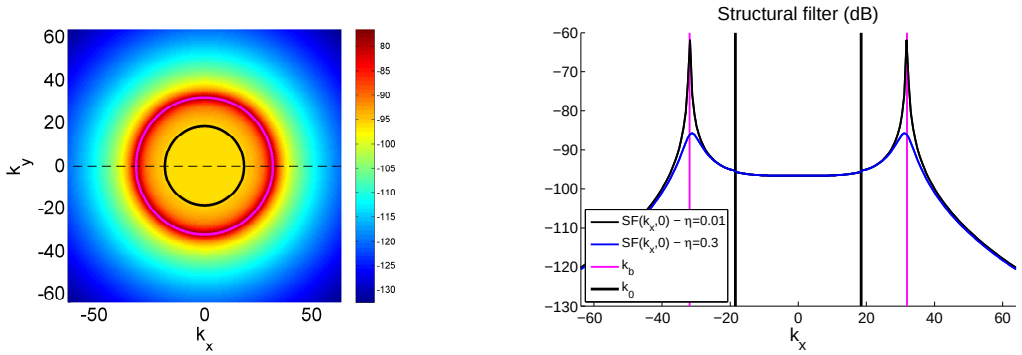

Figure 6: Example of structural filter for an infinite aluminum plate at 1000 Hz in the wavenumber domain: 2D representation (left) and 1D representation along k_x (right).

One can note that this plate acts as a low-pass filter in the wavenumber domain. The cut-off wavenumber is the natural bending wavenumber k_b and the damping factor has only an effect around this wavenumber.

The natural bending wavenumber is :

$$k_b = \sqrt{\omega}\left(\frac{\rho h}{D}\right)^{1/4}, \tag{5}$$

with $\omega = 2\pi f$ the pulsation, ρ the density, D the bending stiffness and h the thickness of the plate. The damping is directly taken into account in the Young's modulus $\tilde{E} = E(1+\mathrm{j}\eta)$.
The critical frequency is given by:

$$f_c = \frac{c_0^2}{2\pi}\sqrt{\frac{\rho h}{D}} \tag{6}$$

where the bending stiffness is $D = Eh^3/(12(1-\nu^2))$.

2.3 Radiation efficiency

The radiation efficiency links the mean quadratic velocity of the structure to the radiated power. For instance, on the reception side:

$$\sigma(k_x, k_y) = \frac{\Pi_{rad}(k_x, k_y)}{\rho_0 c_0 S < V_{rec}^2(k_x, k_y) >}, \tag{7}$$

where ρ_0 and c_0 are the density and the speed of sound of the surrounding fluid (air).

The transfer matrix method has been extended to finite system by using the so-called finite size correction or spatial windowing [5]. This correction consists in computing the radiated power of an infinite structure where only a surface $L_x \times L_y$ contributes to sound radiation. This finite radiation efficiency only depends on the geometry of the multilayer system. This method does not capture the low frequency modal behavior but has proven its relevance on many real cases. This calculation requires a large number of integrals and has been subject of numerous works. In this simple case, the 1D approximation introduced by Vigran [6] is used in order to illustrate the principle on a 1×1 m^2 system.

Note that the radiation efficiency also acts as a low-pass filter in the wavenumber domain with the cut-off frequency k_0.

It is now easy to compute the radiated power $\Pi_{rad}(k_x, k_y)$ from the excitation $F(k_x, k_y)$, the structural filter $SF(k_x, k_y)$ and the radiation efficiency $\sigma(k_x, k_y)$.

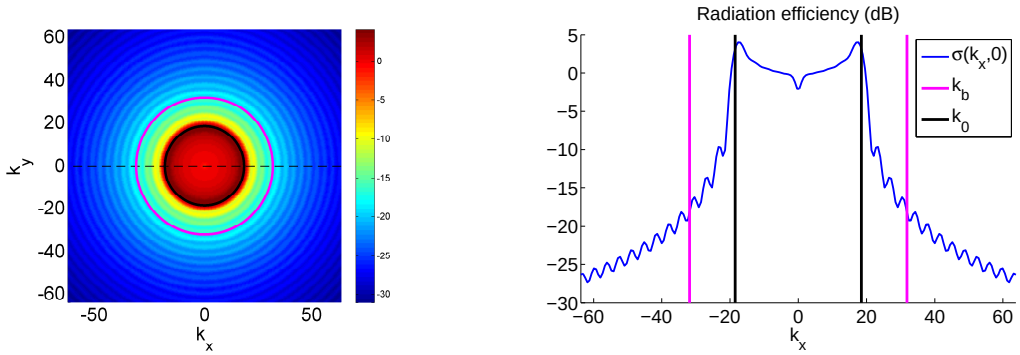

Figure 7: Example of radiation efficiency: 2D representation (left) and 1D representation along k_x (right).

3 ANALYSIS OF MULTILAYER SYSTEM RESPONSES UNDER VARIOUS EXCITATIONS

3.1 Analysis of a simple plate under various excitations

A 4 mm thick aluminum plate (Youngs's modulus $E = 70$ GPa, density $\rho = 2700$ kg.m^{-3}, Poisson's ratio $\nu = 0.3$) is considered. Two damping factors are considered $\eta = 0.01$ and $\eta = 0.05$. For this plate, the critical frequency is $f_c \approx 3100$ Hz.

3.1.1 Diffuse field excitation

The transmission loss of this plate is computed, when submitted to an air-borne diffuse field, for two damping factors. This very classical result shows there is no effect of the damping factor for frequencies lower than the critical frequency.

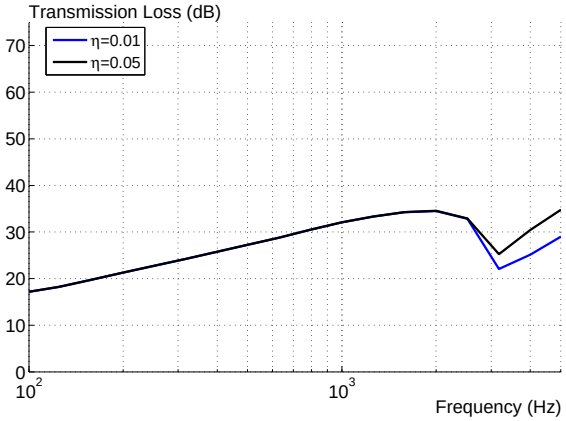

Figure 8: Transmission loss of a simple aluminum plate under **diffuse field excitation** for two damping factors.

Looking at the wavenumber analysis (Fig.9) for frequencies lower than the critical frequency f_c, which means that the acoustical wavenumber k_0 is lower than natural bending wavenumber k_b (see individual graph bottom left), there is no energy around k_b and thus the effect of the damping is weak at these frequencies as mentionned in Sec.2.2.

Obviously, for frequencies higher than the critical frequency f_c, k_0 is larger than k_b which means that there is energy around k_b. Thus there is a significant effect of the damping value on the radiated sound.

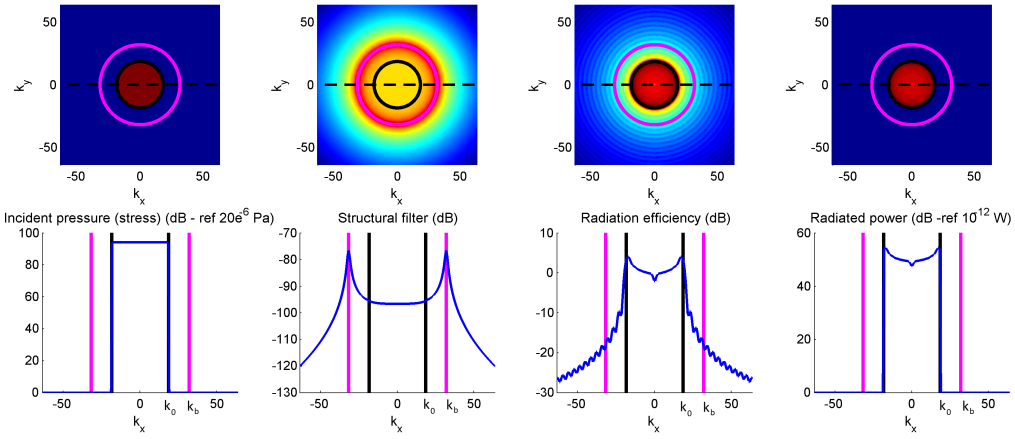

Figure 9: Excitation, structural filter, radiation efficiency and radiated power in the wavenumber domain of an aluminum plate ($\eta = 0.01$) submitted to an **air-borne diffuse field excitation** at 1000 Hz.

3.1.2 Turbulent boundary layer excitation

The same plate is now excited by a turbulent boundary layer. Fig.10 shows that the damping factor affects the transmission loss on the entire frequency range. This can be easily explained in wavenumber domain (see Fig.11) since there is always energy around the natural bending wavenumber k_b. Therefore, the effect of the damping is visible at all frequencies. This effect has been previously observed by Cacciolati *et al.* [7].

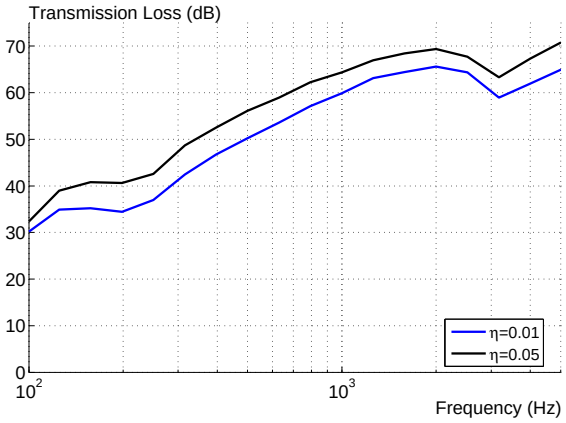

Figure 10: Transmission loss of a simple aluminum plate under **turbulent boundary layer excitation** $U_c = 100$ m.s^{-1}, $\delta = 0.025$ m.

As mentionned in Sec.2.2 the plate acts as a low-pass filter in the wavenumber domain. It has been experimentally observed [8] and this effect can be used for identifying the acoustic component (low wavenumbers) of a turbulent flow exciting a plate by inverting the vibration problem with the so-called force analysis technique (FAT) [9].

3.1.3 Rainfall excitation

The same plate is now submitted to a rainfall excitation (rainfall rate 40 mm/h, drop diameter 5 mm, fall velocity 7 m/s). The rain noise excitation can be predicted according [10]. Fig.12 shows

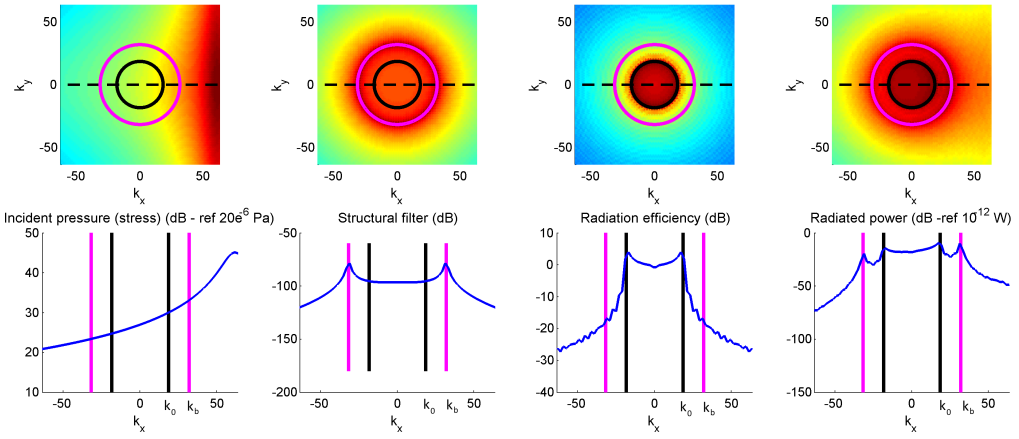

Figure 11: Excitation, structural filter, radiation efficiency and radiated power in the wavenumber domain of an aluminum plate ($\eta = 0.01$) submitted to a **turbulent boundary layer excitation** at 1000 Hz.

that the damping factor affects the radiated intensity level L_i on the entire frequency range. As for the turbulent boundary layer excitation, this can be easily explained in wavenumber domain since there is always energy aroung the natural bending wavenumber k_b which thus implies an effect of the damping factor at all frequencies.

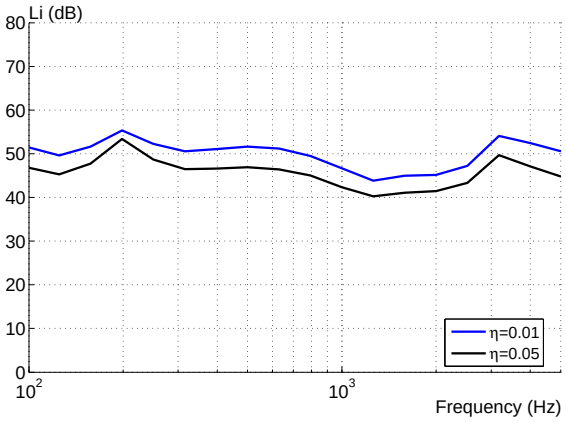

Figure 12. Sound intensity level of a simple aluminum plate under **rainfall excitation**

3.2 Analysis of a double wall partition

A double wall partition with studs (mechanical links) under air-borne diffused field excitation is now considered (see Fig.13). The partition is made of two 12.5 mm thick plasterboards separated by aluminum studs. The 48 mm thick cavity is filled with a glasswool. In this case, air-borne and solid-borne paths have to be taken into account. The air-borne path is computed using the finite size transfer matrix method (FTMM). Davy [11] proposed a way to compute the solid-borne path of such a plate-stud-plate system in parallel to the air-borne path. The total transmission is finally the sum of the air-borne transmission and the solid-borne transmission.
Fig.14 presents the total, the air-borne, and the solid-borne transmission losses of this partition for two damping factors ($\eta = 0.02$ and $\eta = 0.08$) of the plasterboards. The other parameters of plasterboards are: Youngs's modulus $E = 3$ GPa, density $\rho = 700$ kg.m^{-3}, Poisson's ratio $\nu = 0.22$. The critical frequency of such a plasterboard is $f_c = 2450$ Hz.

The airflow resistivity of the glasswool is 11 500 N.s.m^{-4}

The air-borne path shows an effect of the damping factor only for frequencies higher than f_c as observed in Sec.3.1.1.
The solid-borne path shows a strong effect on the entire frequency range. This can be explained by the fact the studs are excited by the first plate (emission side) and act as point forces exciting the second plate (reception side). Point forces excite a wide range of wavenumber as mentionned in Sec.2.1.2. In this case there is energy around the natural bending wavenumber of the second plate and a strong effect of the damping factor is observed.
Finally, the damping factor has an effect on the total transmission loss for frequencies higher than 200 Hz.

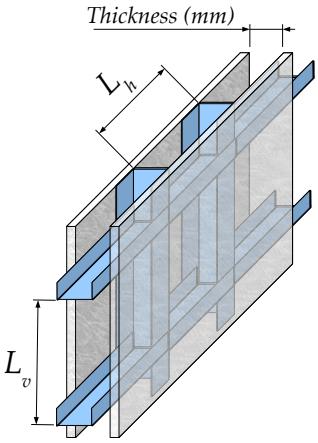

Figure 13. Scheme of double wall partition.

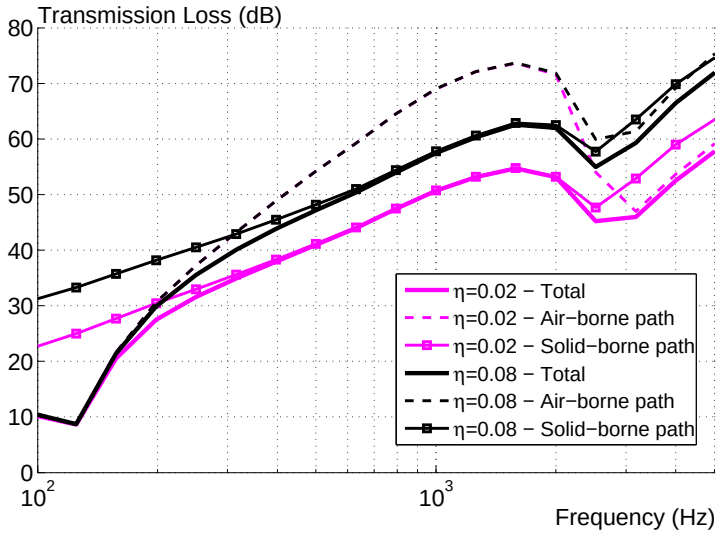

Figure 14. Transmission loss of a double wall partition with studs.

4 CONCLUSION

This paper shows several interest to conduct analysis in the wavenumber domain.
Since each quantity relative to the problem under consideration (excitation, structure response,

radiation efficiency, radiated power) can be expressed in the wavenumber domain, a simple multiplication operation of the excitation by the structural filter and the radiation efficiency allows to compute the radiated power.
This paper shows that the effect of the damping factor of a structure may have a significantly different effect depending on the considered excitation. This effect has been previously observed but can be explained from the wavenumber point of view.
The analysis in the wavenumber domain proves to be useful for interpretating this type of results in the frequency domain.
This type of analysis could be useful for improving indirect identification methods as FAT method.

REFERENCES

[1] G. M. Corcos. The structure of the turbulent pressure field in boundary-layer flows. *Fluid Mech*, 18:353–378, 1964.

[2] M. Goody. Empirical spectral model of surface pressure fluctuations. *AIAA Journal*, 42, 2004.

[3] B. Brouard, L. Lafarge, and J.-F. Allard. A general method of modelling sound propagation in layered media. *J. Sound Vib.*, 1995.

[4] D. Rhazi and N. Atalla. Transfer matrix modeling of the vibroacoustic response of multimaterials structures under mechanical excitation. *J. Sound Vib.*, 329:2532–2546, 2010.

[5] M. Villot, C. Guigou, and L. Gagliardini. Predicting the acoustical radiation of finite size multi-layered structures by applying spatial windowing on infinite structures. *J. Sound Vib.*, 245:433–455, 2001.

[6] T. E. Vigran. Sound transmission in multilayered structures – introducing finite structural connections in the transfer matrix method. *App. Acoust.*, 71:39–44, 2010.

[7] C. Cacciolati, P. Neple, E. Guyader, J.-L. Guyader, and N. Totaro. Comparison of vibroacoustic behaviour of rectangular thin plate excited by a diffuse sound field and a turbulent boundary layer. ICSV, Vienna, Austria, 2006.

[8] F. Chevillotte, Q. Leclere, N. Totaro, C. Pezerat, P. Souchotte, and G. Robert. Identification d'un champ de pression pariètale induit par un écoulement turbulent à partir de mesures vibratoires. CFA, Lyon, France, 2010.

[9] D. Lecoq, C. Pezerat, J.-L. Thomas, and W. Bi. Extraction of the acoustic component of a turbulent flow exciting a plate by inverting the vibration problem. *J. Sound Vib.*, 333 (12):2505–2518, 2014.

[10] D. Griffin and K. Ballagh. A consolidated theory for predicting rain noise. *Building Acoustics*, 19 (4):220–248, 2012.

[11] J. L. Davy. Sound transmission of cavity walls due to structure borne transmission via point and line connections. *J. Ac. Soc. Am.*, 132:814–821, 2012.